Diffuso-kinetic membrane budding dynamics: Electronic Supplementary Material (ESM)

Rossana Rojas Molina[1], Susanne Liese[1], Haleh Alimohamadi[2], Padmini Rangamani[2], and Andreas Carlson[1*]

[1]Mechanics Division, Department of Mathematics, University of Oslo, 0316 Oslo, Norway.
[2]Department of Mechanical and Aerospace Engineering, University of California, San Diego, CA 92093, USA
[*]Email: acarlson@math.uio.no

1 Derivation of the shape equations

The energy functional that describes the membrane is given by:

$$W = B(H - C_0\bar{\sigma})^2 + \lambda + \frac{k_b T}{a_p}\bar{\sigma}(\log\bar{\sigma} - 1) \tag{1}$$

To derive the energy minimizing shape, we define the Lagrangian functional $\mathcal{L}$ as:

$$\mathcal{L} = r\left[\lambda + \frac{k_b T}{a_p}\bar{\sigma}(\log\bar{\sigma} - 1)\right] + rB\left[\frac{1}{2}\left(\frac{\sin\phi}{r} + \phi'\right) - C_0\bar{\sigma}\right]^2 + \Gamma(r' - \cos\phi) \tag{2}$$

The equations that describe the membrane shape are derived from the minimization of a Lagrange functional $\mathcal{L}$ given by Eq. 2 with respect to the functions r and ϕ. These functions are parametrized by the arc-length s. The Euler-Lagrange equations for these functions read:

$$\frac{\partial\mathcal{L}}{\partial r} - \frac{d}{ds}\left(\frac{\partial\mathcal{L}}{\partial r'}\right) = 0 \rightarrow \frac{d\Gamma}{ds} = \lambda + \frac{k_b T}{a_p}\bar{\sigma}(\log\bar{\sigma} - 1) + \frac{M^2}{B} - \frac{M\sin\phi}{r} \tag{3}$$

$$\frac{\partial\mathcal{L}}{\partial\phi} - \frac{d}{ds}\left(\frac{\partial\mathcal{L}}{\partial\phi'}\right) = 0 \rightarrow \frac{dM}{ds} = \frac{\Gamma\sin\phi}{r} \tag{4}$$

We derive a Hamiltonian from the Lagrangian functional in Eq. 2. The total energy of the membrane depends on its area, which is an implicit function of the arc-length s. This implies that the Lagrangian depends on the spatial coordinate s *implicitely* as well. In order to specify the domain where the shape equations are to be solved, the protein concentration $\bar{\sigma}$ must be evaluated on the membrane area. This can be done as the relation $A' = 2\pi r$ provides a one-to-one correspondence between the area A and the arc-length s. Moreover, as the size of the upper limit of the coordinate s is not fixed the following relations are obtained:

$$\frac{\partial\mathcal{L}}{\partial s} = -\frac{d\mathcal{H}}{ds} = 0 \tag{5}$$

$$\mathcal{H}(s_{max}) = 0 \rightarrow \mathcal{H}(s) = 0 \tag{6}$$

The Hamiltonean is given by:

$$\mathcal{H} = -\mathcal{L} + r'\frac{\partial\mathcal{L}}{\partial r'} + \phi'\frac{\partial\mathcal{L}}{\partial\phi'} = 0 \tag{7}$$

Explicitly:

$$\mathcal{H} = r\left[-\left(\lambda + \frac{k_b T}{a_p}\bar{\sigma}(\log\bar{\sigma} - 1)\right) - \frac{M^2}{B} + \frac{\Gamma\cos\phi}{r} + \phi'M\right] = 0 \tag{8}$$

The expression inside the brackets in Eq. 8 vanishes and then we express the terms inside the parenthesis as function of M^2, Γ, r and ϕ. Inserting the resulting expression into Eq. 3 we obtain:

$$\frac{d\Gamma}{ds} = \frac{\Gamma \cos \phi}{r} - \frac{2M \sin \phi}{r} + M\left(\frac{2M}{B} + 2C_0 \bar{\sigma}\right) \tag{9}$$

Next, we write Eq. 3 and Eq. 4 as a function of two new variables Q and T:

$$Q \equiv -\frac{\Gamma \sin \phi}{r} \tag{10}$$

$$T \equiv \frac{\Gamma \cos \phi}{r} \tag{11}$$

Using Eq. 9 these new variables fulfill the following differential equations:

$$\frac{dQ}{ds} = -\frac{M \sin \phi}{r}\left(\frac{2M}{B} - \frac{2 \sin \phi}{r} + 2C_0 \bar{\sigma}\right) - \phi' T \tag{12}$$

$$\frac{dT}{ds} = \frac{M \cos \phi}{r}\left(\frac{2M}{B} - \frac{2 \sin \phi}{r} + 2C_0 \bar{\sigma}\right) + \phi' Q \tag{13}$$

A solution to Eq. 12 and Eq. 13 is given by the following ansatz:

$$Q = -U \sin \phi \tag{14}$$
$$T = U \cos \phi \tag{15}$$

where U satisfies

$$\frac{dU}{ds} = \frac{M}{r}\left(\frac{2M}{B} - \frac{2 \sin \phi}{r} + 2C_0 \bar{\sigma}\right) \tag{16}$$

Finally, the equations that determine the shape of the membrane are given by the ones obtained of the geometry described in Fig. 1 of the Main Text together with Eq. 4 and Eq. 16:

$$\phi' = \frac{2M}{B} - \frac{\sin \phi}{r} + 2C_0 \bar{\sigma} \tag{17}$$

$$r' = \cos \phi \tag{18}$$

$$z' = \sin \phi \tag{19}$$

$$A' = 2\pi r \tag{20}$$

$$M' = U \sin \phi \tag{21}$$

$$U' = \frac{M}{r}\left(\frac{2M}{B} - \frac{2 \sin \phi}{r} + 2C_0 \bar{\sigma}\right) \tag{22}$$

We notice that the shape equations do not depend on the parameter $k_b T$.

2   Boundary conditions

From the geometry used to describe the shape of the membrane, shown in Fig. 1 of the Main Text the following boundary conditions can be extracted:

$$r(s = 0) = 0 \tag{23}$$
$$\phi(s = 0) = 0 \tag{24}$$
$$A(s = 0) = 0 \tag{25}$$

and we define the origin of the z coordinate to be located at $s = 0$:

$$z(s = 0) = 0 \tag{26}$$

However, given the form of the shape equations and its divergent behaviour at $s = 0$ these boundary conditions need to be regularized by doing a Taylor expansion around $s = 0$. Then, we define the boundary condition at $s = \epsilon$ instead of $s = 0$, where $\epsilon \ll 1$:

$$r(\epsilon) \approx r(0) + \epsilon r'(0) = \epsilon \tag{27}$$

$$\phi(\epsilon) \approx \phi(0) + \epsilon \phi'(0) \equiv \epsilon c_1 \tag{28}$$

$$A(\epsilon) \approx A(0) + \epsilon A'(0) + \frac{\epsilon^2}{2} A''(0) = \pi \epsilon^2 \tag{29}$$

$$z(\epsilon) \approx z(0) + \epsilon z'(0) + \frac{\epsilon^2}{2} z''(0) = \frac{c_1}{2} \epsilon^2 \tag{30}$$

$$M(\epsilon) \approx B(c_1 - C_0 \bar{\sigma}(\epsilon)) \tag{31}$$

where c_1 is defined as the mean curvature at $s = \epsilon$ and results from solution of the ODEs. Additionally, we impose that at the far boundary s_{max} the membrane is nearly flat which implies:

$$\phi(s_{max}) = 0 \tag{32}$$

To find a boundary condition for the function U, we use the expression for the Hamiltonean in Eq. 8. This equation holds identically assuming that $r(s = 0) = 0$, and it holds for $s = s_{max}$ only if the term in brackets vanishes. The equation 32 allow us to assume that the mean curvature and the bending moment M vanish at the far boundary. With these assumptions, we can find a relation for $U(s_{max})$:

$$U(s_{max}) = \lambda + \frac{k_b T}{a_p} \bar{\sigma}(\log \bar{\sigma} - 1) \approx \lambda \tag{33}$$

where σ is evaluated at s_{max}. As we are considering a large spacial domain, the protein concentration at the far boundary satisfies $\bar{\sigma}(s_{max}) \approx 0$, and then $U(s_{max})$ can be written as in eq. 33. In this way, we have a system of 6 coupled ordinary differential with the boundary conditions in Eq. 27-33 and the parameter c_1.

3 Non-dimensional analysis

Assuming that the characteristic length of the system, L, is given by the typical vesicle size, we can non-dimensionalize the shape equations and the evolution equation for the protein concentration σ as follows:

$$\bar{s} = \frac{s}{L}, \qquad \bar{r} = \frac{r}{L}, \qquad \bar{z} = \frac{z}{L}, \qquad \bar{M} = \frac{ML}{B}, \qquad \bar{C}_0 = C_0 L$$

$$\bar{U} = \frac{UL^2}{B}, \qquad \bar{Q} = \frac{QL^2}{B}, \qquad \bar{\lambda} = \frac{\lambda L^2}{B}, \qquad \bar{\sigma} = \frac{\sigma}{\sigma_m}$$

$$\bar{t} \equiv \frac{t}{\tau_D} = \frac{tD}{L^2}, \qquad \bar{\Lambda} = \frac{\Lambda B}{L^2 D} = \frac{B}{k_b T} \frac{a_p}{L^2}$$

Substituting the dimensional quantities in terms of the non-dimensional variables and then dropping all the bars, the evolution equation can be written in dimensionless form as

$$\bar{\sigma}_t - \frac{1}{r}(r(\sigma' + 2\bar{C}_0 \bar{\Lambda} \bar{\sigma} \bar{Q}))' = \frac{\tau_D}{\tau_{on}} \Theta(H - H_0) - \frac{\tau_D}{\tau_{off}} \bar{\sigma} \tag{34}$$

where τ_{on} and τ_{off} define the time scales of recruitment and detachment, respectively, and are given by:

$$\tau_{on} = \frac{1}{c_p k_{on}}, \qquad \tau_{off} = \frac{1}{k_{off}}$$

where c_p is the typical protein concentration on the bulk surrounding the membrane and k_{on} is the affinity between the proteins and the membrane. Further, we define the ratio between the time scales as:

$$K_1 \equiv \frac{\tau_D}{\tau_{on}} \qquad K_2 \equiv \frac{\tau_D}{\tau_{off}}$$

where $\tau_D = \frac{L^2}{D}$ is the typical diffusive time scale on a biological membrane. With these definitions we recover Eq. 15 of the Main Text.

3.1 Numerical implementation

To solve numerically the shape equations we used the solver bvp4c in Matlab and the evolution equation of the protein concentration was solved using a finite difference discretization in time and space, where the spatial derivatives where computed by a centered-difference scheme and the time derivative by a backward scheme. The steps to solve the coupled equations are summarised as follows:

1. Give an initial protein concentration $\bar{\sigma}_0$, for example a Gaussian profile, with small amplitude.

2. Solve the associated shape equations using bvp4c in Matlab.

3. With the geometry given by the solution of the shape equations, solve the difusso-kinetic equation to obtain the protein concentration at a later time step, namely, $\bar{\sigma}$, using as initial density $\bar{\sigma}_0$.

4. Solve the shape equations with the new protein concentration $\bar{\sigma}$.

5. Update the initial protein concentration, $\bar{\sigma} \rightarrow \bar{\sigma}_0$

6. Iterate over the steps 3 to 5, until the formation of a bud neck with almost vanishing width is reached. In this case the shape equations and the evolution equation for $\bar{\sigma}$ becomes singular and the numerical solver cannot provide a valid numerical solution. As explained in the main text, we will consider the evolution of the membrane shape until the time t_{cut}, at which the membrane neck has a small but finite width, equal to the membrane thickness.

4 Validity of the solutions given by the shape equations.

To show that the shapes obtained as a result of the integration of the shape equations, Eq. 17-22 do correspond to a minimized energy we consider the case of zero surface tension, namely $\lambda = 0$ in the energy functional given by Eq. 1. In this case, the bending moment M given in Eq. 21 should vanish, which implies that the mean curvature of the membrane follows the spontaneous curvature imposed by the proteins. Hence, a simplified set of equations can be obtained by setting $M = 0$. As a consequence, $U = 0$. These equations are:

$$\phi' = -\frac{\sin\phi}{r} + 2C_0\bar{\sigma} \tag{35}$$

$$r' = \cos\phi \tag{36}$$

$$z' = \sin\phi \tag{37}$$

$$A' = 2\pi r \tag{38}$$

with the following boundary conditions:

$$r(\epsilon) = \epsilon$$
$$\phi(\epsilon) = C_0\bar{\sigma}(A = 0)\epsilon$$
$$A(\epsilon) = \pi\epsilon^2$$
$$z(\epsilon) = \frac{C_0\bar{\sigma}(A = 0)}{2}\epsilon^2$$

In Fig. 1a we compare the shapes obtained at $t = t_{cut}$ by solving the full set of equations, Eq. 17-22 (set of equations 1), and the simpler equations given by Eq. 35-38 (set of equations 2) for $K_1 = 2.25$ and $H_0 = 0.015$. The shapes obtained are very similar, indicating that the assumption of vanishing bending moment, $M = 0$, when the surface tension vanishes is correct. In addition, in Fig. 1b we show that by solving the set of equations 1, the bending moment is zero.

4
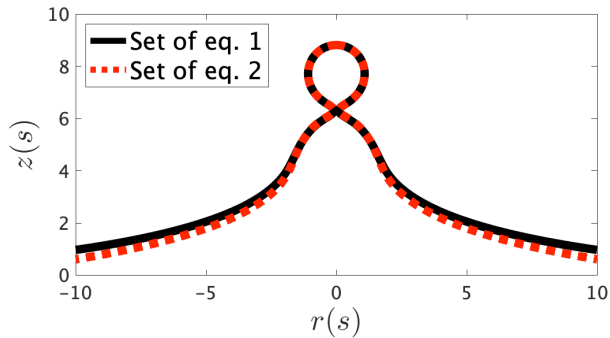
(a) Comparison between the shapes obtained by solving the set of equations 1 and 2.
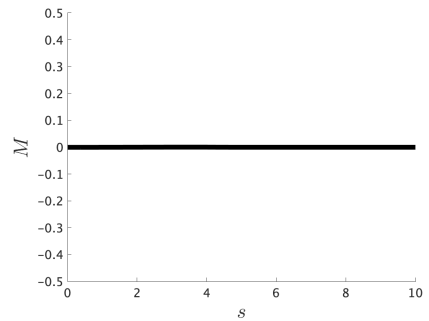
(b) The bending moment $M(s)$ obtained by solving the set of equations 1.

Figure 1: Verification of the validity of the solutions given by the shape equations (set 1), for the particular case of vanishing surface tension, $\lambda = 0$. The shape obtained agrees well with the solution given by the simplified equations (set 2). The bending moment $M(s)$ obtained as a solution of the shape equations vanishes, as shown in fig. 1b.

4.1 Effect of the initial protein density

In all the simulations, we have assumed that the initial protein density is given by a Gaussian profile, $\bar{\sigma}(s, t = 0) = \sigma_0 e^{-(s/0.3)^2}$, where σ_0 measures the amplitude of the initial density. In all the results presented in the main text we have chosen $\sigma_0 = 0.1$. Given that the recruitment term depends on the mean curvature via a cutoff function, the membrane should have initially a small but finite deformation to trigger the recruitment. Then it is expected that if the initial protein density is too small, the membrane will not evolve into a budded shape. To see the effect of the parameter σ_0 on the membrane shape dynamics, we chose $K_1 = 9$ and $H_0 = 0.15$ and varied the amplitude of the initial density. If $\sigma_0 = 0.03$, *i.e*, almost one order of magnitude smaller than the one we have considered, the membrane remains flat, as shown in Fig. 2a. However, with an initial amplitude of $\sigma_0 > 0.03$ the membrane evolves into a budded shape, similar to the one obtained when $\sigma_0 = 0.1$. In Fig. 2b we show the dependence between the time at which the neck width equals the membrane thickness, t_{cut}, and the amplitude of the initial protein density, σ_0, where it is observed that the initial amplitude σ_0 has a small effect on t_{cut}. Hence, the parameter σ_0 plays a minor role in the budding dynamics.
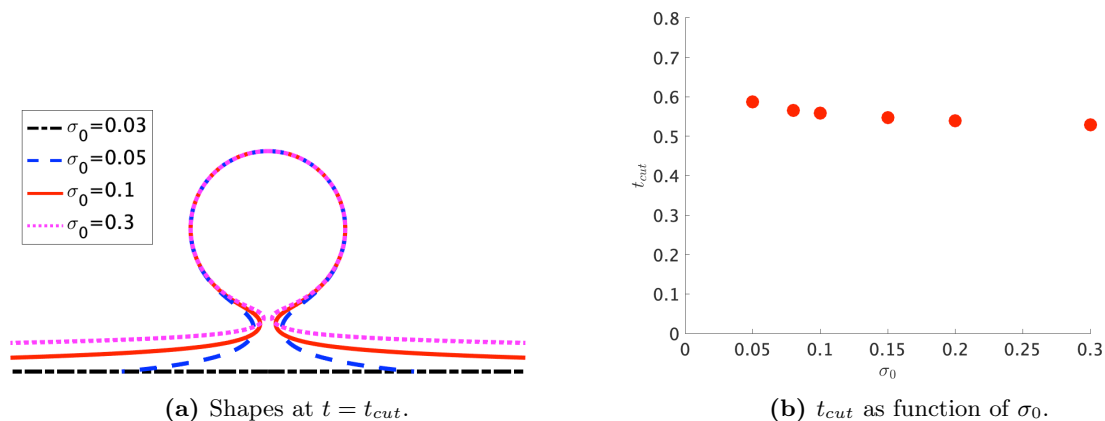
(a) Shapes at $t = t_{cut}$.
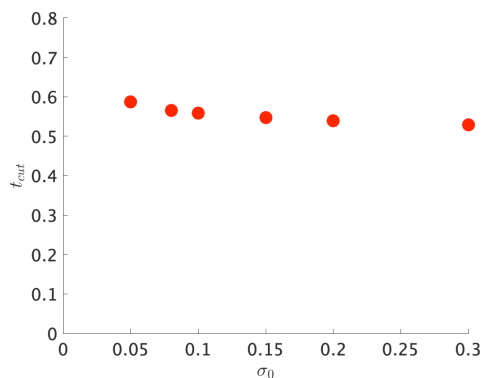
(b) t_{cut} as function of σ_0.

Figure 2: (a) Comparison of the shapes obtained at $t = t_{cut}$ for $K_1 = 9$ and $H_0 = 0.15$, when $\sigma_0 = 0.1$. The amplitude of the initial protein density does not have a strong influence in the final membrane shape, provided $\sigma_0 > 0.03$. If $\sigma_0 < 0.03$ the membrane shape does not evolve into a budded structure. (b) The scission time t_{cut} as a function of the initial density amplitude, σ_0, showing that indeed t_{cut} is only slightly modified by the parameter σ_0. Then, this parameter does not play a key role in the membrane budding dynamics.

4.2 Regularising the Heaviside for the recruitment model

In the main text we have assumed that the protein recruitment depends on the membrane curvature via a cut-off or Heaviside function that is piece-wise constant, giving a finite and constant on rates when the membrane mean curvature exceeds a threshold $H > H_0$, and vanishing rate when $H < H_0$. Instead of a Heaviside function an hyperbolic tangent function can be used, $i.e$, $\Theta(H - H_0) \rightarrow 0.5(1 + \tanh a(H - H_0))$, where a determines the steepness of the tanh function. To mimic the Heaviside, a should be large enough, to ensure that if $H < H_0$ the recruitment vanishes. The parameters K_1 and K_2 have a clear physical interpretation, as on and off rates. Other models for protein recruitment could be considered. For example, one could assume that the recruitment term is proportional to the mean curvature, $\sim \beta H$, where β is a constant of proportionality. Nevertheless, β might not have a straightforward physical interpretation, and to address the general effect of changing the recruitment model is beyond the scope of this work. In Fig. 3a we show the comparison between the shapes obtained for the Heaviside and tanh, for $K_1 = 2.25$ and $H_0 = 0.015$, corresponding to $t = t_{cut}$. We observe that the Heaviside and the tanh model give very similar shapes when $a > 300$ and the protein profiles $\bar{\sigma}$ as a function of the area A are nearly identical to the Heaviside solution (Fig. 3b). Only when the tanh function becomes wide $a < 300$ the results start to deviate from the solution from the Heaviside as recruitment of proteins have "leaked" over a larger area due to the width of the tanh-function.

(a) Shapes at $t = t_{cut}$ for $K_1 = 2.25$ and $H_0 = 0.015$. **(b)** $\bar{\sigma}(A)$ for the shapes in Fig. 3a.
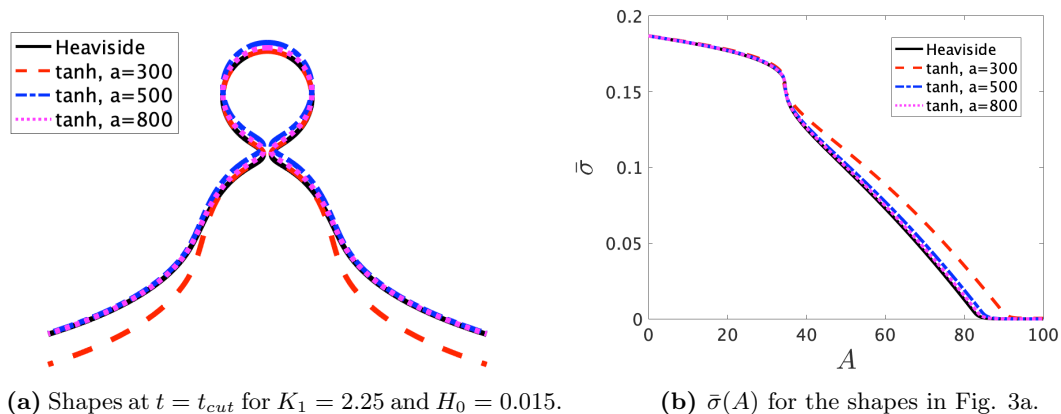
Figure 3: (a) Shapes obtained with the Heaviside model and its regularized version $\sim 0.5(1 + \tanh a(H - H_0))$ at $t = t_{cut}$ for $H_0 = 0.015$ and $K_1 = 2.25$. The shapes are similar, provided that the tanh is steep enough. If $a < 300$ the shapes differ. (b) The protein density $\bar{\sigma}$ as a function of the area A, associated to the shapes in Fig. 3a. If the tanh function is not steep enough ($a < 300$), the density $\bar{\sigma}$ start to differ, as the recruitment term leaks to a larger membrane area as the tanh function becomes wide.

5 Estimation of the interaction and gradient terms in the energy functional

According to Eq. 1, we are considering an energy functional where interaction terms $\sim b\bar{\sigma}^2$ and gradient terms $\sim b(\nabla\bar{\sigma})^2$ are absent, as we have assumed that the interaction between proteins b is weak. This choice a priori is arbitrary, as in general these terms should be present. However, it is illustrative to estimate the relative importance of these terms respect to the bending energy and the entropy. In order to do this, for simplicity we will assume that $\lambda = 0$. Following the result of the previous section, if the surface tension vanishes the bending moment and hence the bending energy vanishes for any given protein concentration profile (see Fig. 1b). We will assume that the protein concentration is one of the solutions obtained from the numerical simulations at a given time step, for $K_1 = 2.25$ and $H_0 = 0.015$, shown in Fig. 4a.

It has been estimated theoretically and experimentally that the interaction potential is of the order of $2k_bT$ (1; 2), which in practice is considerably smaller than the typical bending energy of the membrane. Then the interaction potential should satisfy $b \ll B$. In Fig. 4b we plot the adimensional entropic term $\frac{k_bT}{B}\frac{L^2}{a_p}\bar{\sigma}(\log(\sigma) - 1)$, the interaction term $-\frac{b}{B}\frac{L^2}{a_p}\bar{\sigma}^2$ and the gradient term $\frac{b}{B}(\nabla\bar{\sigma})^2$ assuming that the ratio $\frac{b}{B} = \frac{1}{10}$. We can observe that in this case the entropy dominates over the interaction and the gradient terms. Hence, it is reasonable to neglect these terms in the energy functional.
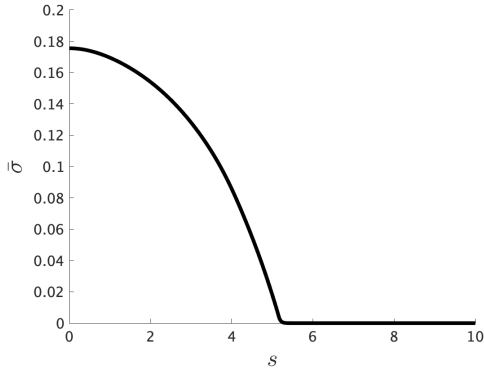
(a) A protein profile obtained from numerical simulations, for $K_1 = 2.25$ and $H_0 = 0.015$.
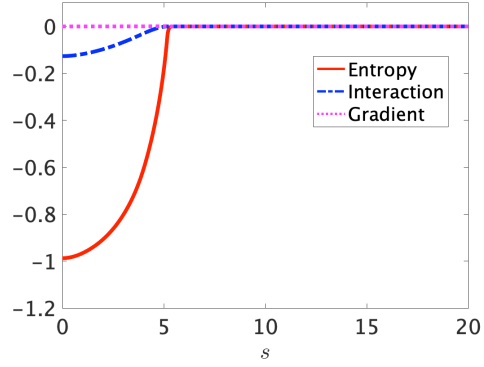
(b) Comparison between the entropy and the interaction term for the protein profile in fig. 4a

Figure 4: Estimation of the contributions to the energy arising from the entropy and interaction between proteins. Assuming that the ratio $\frac{b}{B} = \frac{1}{20}$, the interaction and gradient terms have a small contribution to the energy.

6   The effect of surface tension in the membrane shape evolution

The surface tension influences the budding time and the shape of the forming vesicle. In order to establish the effect of the surface tension in the membrane dynamics we fix the parameters K_1 and H_0 and change the the parameter λ. As λ increases, the numerical calculations become challenging and exploring the effect of the surface tension on the membrane shape evolution is limited to very small values of λ. The dependence of z_{max} with respect to time is shown in Fig. 5a for some values of λ. One of the effects of having surface tension in the system is that the variable z_{max} defined in the main text ceases to have an oscillatory behaviour after a certain value of λ, which implies that the formation of pearl structures is prevented in general. The budding time t_{bud} is defined respect to the local minimum of $z_{max}(t)$, which, following the discussion presented in the main text, correspond to the formation of an Ω-shape. The budding time t_{bud} as a function of λ is shown in Fig. 5b, where it can be observed that the surface tension delays the formation of the bud, as t_{bud} increases if the surface tension becomes larger.
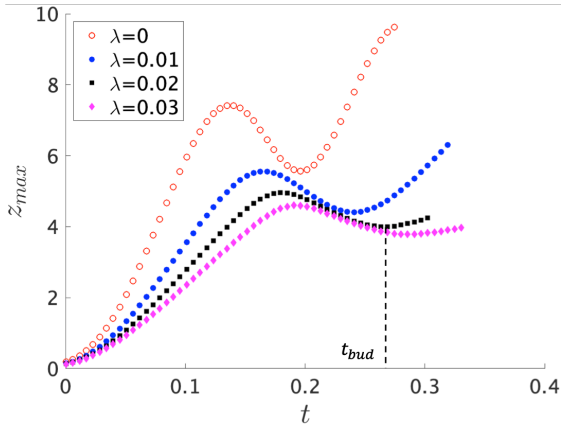
(a) $z_{max}(t)$ for different values of λ.
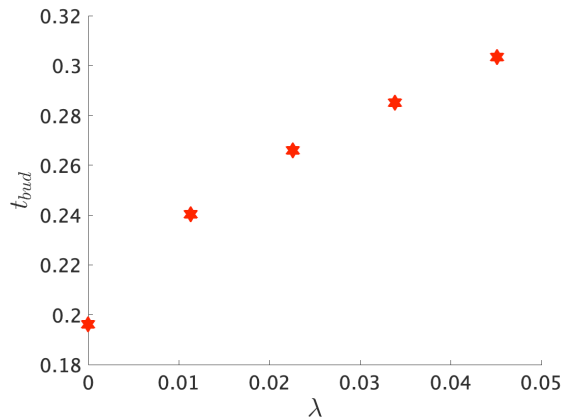
(b) t_{bud} as a function of λ.

Figure 5: The effect of the membrane tension in its shape evolution. Fig. 5a shows the evolution in time of the height of the budding structure z_{max}. This function does not exhibit oscillations in general, as in the case where $\lambda = 0$. Hence, the formation of pearls is prevented in most cases. In Fig. 5b the budding time, t_{bud} is plotted as function of the tension λ. The budding time corresponds to the first local minimum of z_{max}. t_{bud} increases as the surface tension becomes larger. This indicates that the surface tension delays the budding process. In all simulations $K_1 = 2.25$ and $H_0 = 0.015$.

To further characterise the effect of surface tension on the membrane shape, we compare the shapes obtained when $\lambda = 0.04$ and the ones corresponding to $\lambda = 0$, at given times. This comparison is shown in Fig. 6, where is shown that at the scission time $t = t_{cut}$ corresponding to vanishing surface tension, $\lambda = 0$, $H_0 = 0.015$ and $K_1 = 2.25$, the membrane

under the effect of surface tension exhibits quite different shapes. In general, the surface tension favors the formation of budding structures with small height, as compared with the shapes when $\lambda = 0$.

(a) $t = 0.2t_{cut} = 0.05$.   (b) $t = 0.5t_{cut} = 0.13$.   (c) $t = t_{cut} = 0.25$.
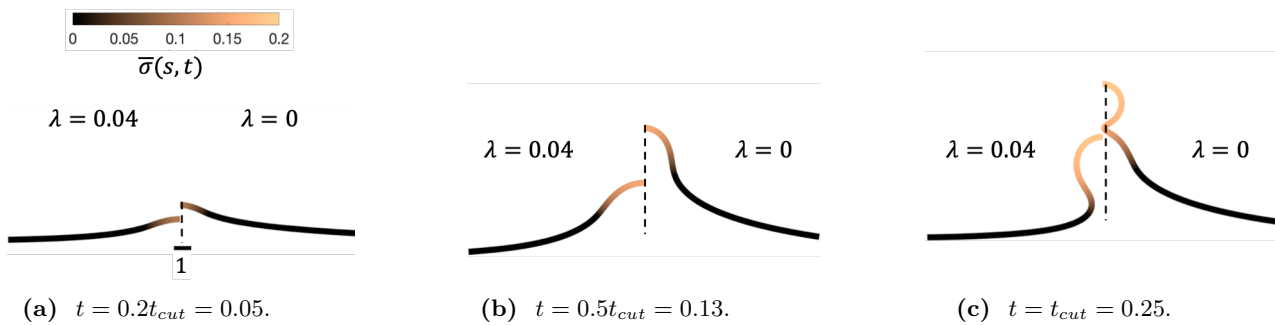
Figure 6: Comparison between the shapes obtained when the surface tension is zero, $\lambda = 0$ and $\lambda = 0.04$ at three different snapshots in time defined respect to t_{cut} discussed in the main text, when the dimensionless rate coefficient is $K_1 = 2.25$ and the threshold for protein recruitment is $H_0 = 0.015$. As we march forward in time the membrane deforms from a nearly flat membrane (not shown) into a pit-shape for both values of λ (a), but the shapes start to differ visibly at a later time ((b) and (c)) and at $t = t_{cut}$ a pearl structure is already formed when $\lambda = 0$ but only a single bud is formed when $\lambda = 0.04$ (c). The color bar represents the protein density $\bar{\sigma}(s,t)$. A finite but small value of λ has the overall effect of reducing the height of the budding structure and preventing the formation of pearls. The scale bar is the dimensionless unit length of the system, equivalent to $L = 50$nm.

References

[1] I. Casuso, P. Sens, F. Rico, and S. Scheuring, "Experimental Evidence for Membrane-Mediated Protein-Protein Interaction," *Biophysical Journal*, vol. 99, no. 7, pp. L47–L49, 2010.

[2] H. Zhou, "Enhancement of protein-protein association rate by interaction potential: Accuracy of prediction based on local Boltzmann factor," *Biophysical Journal*, vol. 73, no. 5, pp. 2441–2445, 1997.